Detection and Localization of Steel Intraocular Foreign Bodies Using Computed Tomography

A Comparison of Helical and Conventional Axial Scanning

Joseph G. Chacko, MD,[1] Ramon E. Figueroa, MD,[2] Maribeth H. Johnson, MS,[3] Dennis M. Marcus, MD,[1] Steven E. Brooks, MD[1]

Purpose: To compare the sensitivity and specificity of detection, and accuracy of localization, of small steel intraocular and episcleral foreign bodies, using conventional axial and helical computed tomographic scanning in an experimental model.

Methods: Small steel foreign bodies ranging in size from 0.048 to 0.179 mm^3 were placed in intraocular and episcleral locations in eye bank eyes mounted in the orbits of a human skull and scanned using helical and conventional axial techniques. Helical scanning was performed using 1-mm and 3-mm thick sections. Conventional axial scanning was performed using 3-mm thick sections. Images were reviewed by masked observers to determine sensitivity, specificity, and accuracy of localization for each imaging method.

Results: Steel foreign bodies as small as 0.048 mm^3 were detectable with each scanning protocol. Although the helical scans appeared to provide higher levels of sensitivity compared to conventional axial scanning, the difference in outcome between the scan types was not statistically significant. Sensitivity was dependent on the size of the foreign body and ranged from 45% to 65% for the smaller ones (<0.06 mm^3) to 100% for the larger ones (>0.06 mm^3). Multiplanar reformatting of images was helpful in achieving optimal accuracy.

Conclusion: In an experimental model of steel intraocular foreign body, helical computed tomographic scanning provided images of high quality similar to that of conventional axial scanning. *Ophthalmology 1997;104:319–323*

Originally received: February 8, 1996.
Revision accepted: September 5, 1996.

From the Departments of [1]Ophthalmology, [2]Neuro-Radiology, and the [3]Office of Biostatistics, Medical College of Georgia, Augusta.

Dr. Chacko is currently affiliated with the United States Public Health Service/Indian Health Service, Phoenix, Arizona.

Presented in part at the 19th Annual Medical College of Georgia Ophthalmology Resident–Alumni Meeting, Augusta, Georgia, March 1995.

Supported in part by an unrestricted departmental award from Research to Prevent Blindness, Inc, New York, New York.

Reprint requests to Steven E. Brooks, MD, Department of Ophthalmology, Medical College of Georgia, 1120 15th St, Augusta, GA 30912.

The detection and accurate localization of intraocular foreign bodies (IOFBs) is critical for the appropriate management of ocular trauma. This evaluation often is difficult because of media opacities such as vitreous hemorrhage or cataract and the presence of associated ocular injuries that may render the eye unstable for thorough ophthalmoscopic and biomicroscopic examination. In addition, small IOFBs may lodge in regions of the eye not directly visualizable (e.g., ciliary body) on ophthalmoscopic examination.

Conventional computed tomographic (CT) scanning of the orbits generally is regarded as the diagnostic method of choice for the detection of metallic IOFBs.[1–4] It provides sensitivity and specificity superior to echography

and film radiographic examinations. The use of magnetic resonance imaging for the detection of IOFBs has been limited because of concern about potential movement of ferromagnetic IOFBs and the damage that this may cause to delicate intraocular tissues.[5]

Although limitations exist,[1,2,6] conventional CT scanning has been refined and improved significantly since its invention. Not only has the imaging resolution been increased, but currently available software and hardware allow for the generation of novel 2- and 3-dimensional (3D) images of the tissues studied[3] using reformatted data acquired from serial tomographic sections. Despite these improvements, the use of conventional CT to detect IOFBs may be limited by its relatively long acquisition time per study, image degradation from eye motion, and limited quality of computer-reformatted images in sagittal or oblique planes.

Helical CT, also known as spiral CT, is a recently developed design of CT equipment and scanning software in which the region of interest is sampled in a seamless fashion as it is moved across an x-ray beam from a continuously rotating x-ray tube within the CT gantry.[7,8] Fast data acquisition allows the entire volume of tissue to be scanned and imaged with minimal motion artifacts. The acquired image data then may be postprocessed to decrease slice thickness or change the bone–soft tissue rendering with minimal loss of image quality. The continuity of the image data set and postprocessing flexibility also allow for the generation of images along any 2-dimensional axis, as well as 3D images, which have spatial resolution nearly equivalent to that of the original axial image. Although multiplanar reformatting also is possible with conventional CT scanning, the reformatted images often have spatial resolution inferior to that of the original images because of discontinuities in the data set. Although such discontinuities can be avoided by obtaining overlapping image slices, this process is time consuming and adds additional radiation exposure to the eye.

Because of its special features, helical CT may offer advantages over conventional CT in the detection and localization of metallic IOFBs. To investigate this postulate, we performed an experimental masked prospective study comparing the sensitivity and specificity of conventional and helical CT methods in the detection and localization of small steel IOFBs in human cadaver eyes.

Methods

Preparation of Cadaver Eyes

Ten whole globes designated for research use only were obtained from the Medical College of Georgia Eye Bank. Each globe was inspected grossly to ensure that no significant structural abnormalities were present. Intraocular volume was restored by injection of water into the vitreous cavity through the pars plana via a 30-gauge needle.

Placement of Metallic Foreign Bodies

Small fragments of steel were obtained by cutting 0.39-mm diameter steel wire into various lengths with a wire cutter, ranging from 0.4 to 1.5 mm (Fig 1). The length and diameter of each fragment were determined by measuring these dimensions under a microscope on a Neubauer Hemocytometer grid (American Optical, Southbridge, MA). The volume of the fragments ranged from 0.048 to 0.179 mm^3.

Figure 1. Examples of metallic (steel) foreign bodies used in experiment. The diameter of each is 0.39 mm. The lengths range from 0.4 to 1.5 mm. The corresponding volumes range from 0.048 to 0.179 mm^3. A United States dime is shown for size comparison.

The study was designed to allow the placement of up to four (total intraocular plus episcleral) foreign bodies (FBs) per globe. For the purpose of standardizing the positioning of the FBs, each eye conceptually was divided into eight sectors by simultaneous equatorial division along the sagittal, coronal, and transverse (axial) planes. The FBs could be placed in any of the eight sectors, either intraocularly or extraocularly (episcleral), with a maximum of one FB per sector and four FBs per eye. Although this design permitted up to a total of 40 IOFBs to be placed in the 10 eyes studied (4 per eye), only 25 FBs actually were used.

Intraocular placement of FBs was accomplished by making a tiny incision in the sclera with a scalpel blade directly over the desired position. The steel fragment then was placed into the retina–choroid using jeweler's forceps. Episcleral FBs were placed against the superficial episcleral tissue using jeweler's forceps. All globes were marked at the 12 o'clock limbus using a surgical marking pen. All FBs were placed by the same investigator (JGC).

Preparations of Cadaver Skull

A dried human skull with the top of the calvarium removed was borrowed from the Anatomy Department of the Medical College of Georgia. It was prepared as described by Tate and Cupples[1] with minor modification. To simulate brain tissue in the anterior cranial fossa, this space was filled with paraffin, which has an x-ray attenuation coefficient similar to brain parenchyma.[1] The orbits were filled with lipid-rich vegetable shortening to simulate orbital fat. The prepared globes were placed into the

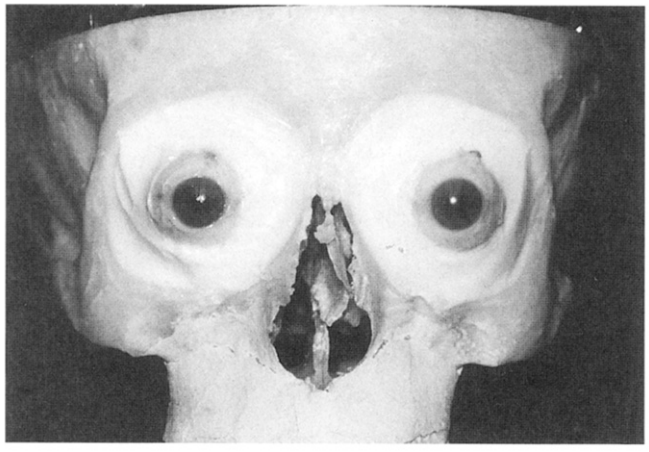

Figure 2. Dried human skull, orbits filled with lipid-rich vegetable shortening, into which human cadaveric eyes containing foreign bodies were positioned for scanning.

orbits in their correct anatomic position (Fig 2). The entire skull was immersed in a water bath, positioned vertex down, for scanning.

Scanning Techniques and Parameters

A total of 5 pairs of eyes (10 eyes total) were scanned on a state-of-the art helical CT scanner (Hi-Speed Advantage CT, General Electric Medical Systems, Milwaukee, WI). Image data were stored and displayed on a free-standing 3D workstation for multiplanar reformatting and viewing (Allegro Workstation, ISG Technologies, Toronto, Canada). Three different scanning protocols were used on each specimen: (1) conventional CT of the orbit in the axial plane using 3-mm thick images at 3-mm spacing; (2) helical scanning in the axial plane with 3-mm thick images at 3-mm table increment (pitch 1:1); and (3) helical scanning in the axial plane with 1-mm thick axial images at 1-mm table increment (pitch 1:1). All series were acquired in bone algorithm and reprocessed in soft tissue.

The 3-mm helical data set was postprocessed in the helical CT computer immediately after acquisition to generate continuous 1-mm partitions. The conventional CT 3-mm images, the postprocessed helical 3-mm images, and the helical 1-mm images were transferred electronically to the 3D workstation for separate viewing in identical conditions. Images were coded so as to give no direct information about the specimen under study. Only the investigator who prepared the specimens (JGC) was aware of the code and the number and position of the FBs in each specimen.

Image Analysis

Images were presented independently to the reviewer, in random order by eye and scanning protocol, by the same investigator who placed the FBs. A total of 15 scans were reviewed. The reviewer was allowed to adjust the image parameters (e.g., orientation, contrast, magnification) using the workstation software to obtain the greatest possible accuracy. Using a separate form for each scan, the reviewer recorded the number and position of any FBs found in each eye. The reviewer was not given prior knowledge of the number or position of FBs present in a given scan and was not permitted to return to previously reviewed images.

Statistical Analysis

The results obtained from the reviewer were used to determine sensitivity and specificity of FB detection and localization and their relation to size of the FB and scanning protocol. The overall sensitivity for detecting the FBs was determined as the proportion of FBs identified by the scan to the total number of FBs present (n = 25). The FBs also were divided into two groups based on size, and the sensitivity of each scanning protocol was determined for each size category. Those FBs greater than 0.06 mm^3 (n = 15) were classified as large, and those FBs less than 0.06 mm^3 (n = 10) were classified as small. The FBs also were classified as intraocular (n = 12) or episcleral (n = 13), and the sensitivity for correct localization was determined for each category based on those FBs that were detected. A binomial 95% confidence interval was calculated for each sensitivity that was not equal to 100%.

For each scanning protocol, Fisher's exact test was used to compare the sensitivity for detecting FBs based on size. Fisher's exact test also was used for each scan to determine if there was a difference in accuracy of localization between intraocular and episcleral FBs. An exact McNemar test was used to make paired comparisons between the three different scanning protocols of their sensitivity for detection and localization of the FBs. Separate comparisons for sensitivity of FB detection were made based on all FBs (n = 25), small FBs (n = 10), and large FBs (n = 15). Comparisons for accuracy of localization were made based only on those FBs detected by each of the two scanning protocols being compared.

Results

A total of 25 FBs were placed in the 10 orbits studied. The overall sensitivity of detection was 88% for the helical 1-mm scans, 84% for the helical 3-mm scans, and 80% for the axial 3-mm scans. These differences in sensitivity among the scanning protocols were not found to be statistically significant, but the relatively small sample size did not provide sufficient power to state this with certainty. The respective specificities for the three protocols were 99%, 100%, and 100%. Again, there appeared to be no statistically significant difference among the three groups.

As expected, the detection sensitivity was dependent on the size of the FB. Ten FBs were 0.06 mm^3 or smaller, whereas 15 were larger. The sensitivity for detection of the smaller FBs was 70% for the helical 1-mm, 60% for the helical 3-mm, and 50% for the axial 3-mm scans. Although the differences between the different scanning protocols suggest a significant trend, the small sample size did not provide the statistical power required to con-

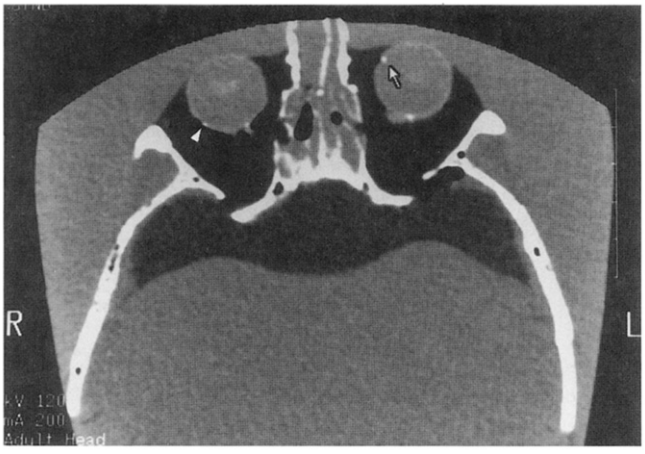

Figure 3. Axial image obtained from helical scan (1-mm partition, 1:1 pitch) shows 0.048-mm^3 intraocular steel foreign body in anterior aspect of the left globe (arrow). A small area of dystrophic scleral calcification is seen in the right globe (arrowhead).

firm this. For the larger FBs (>0.06 mm^3), the sensitivity was 100% for all scan types. The difference in sensitivity for detecting large versus small FBs was statistically significant ($P < 0.05$ for helical 1 mm, $P < 0.02$ for helical 3 mm, and $P < 0.005$ for axial 3 mm) for each scanning protocol.

The overall sensitivity for correctly localizing the detected FBs as intraocular or episcleral was 91% for the helical 1-mm scan, 86% for the helical 3-mm scan, and 85% for the axial 3-mm scan. These differences did not reach statistical significance. Although FBs less than 0.06 mm^3 comprised only 22% to 30% of the FBs detected, depending on scan type, they accounted for 63% of the errors in localization overall. There also appeared to be a slightly increased frequency of errors in localizing IOFBs compared to episcleral FBs, even when FB size was taken into account, although this difference was not statistically significant.

Discussion

Accurate detection and localization of metallic IOFBs is essential for the appropriate management of ocular trauma. Our data suggest that helical CT scanning may be comparable or superior to conventional axial scanning for accomplishing this goal. In this study, the helical 1-mm scans appeared to provide the highest sensitivity and specificity. This finding is not surprising given that the resolution of CT scanning is highly dependent on slice thickness, with thinner cuts providing higher resolution. Interestingly, however, in the context of our experimental model, the conventional 3-mm axial and 3-mm helical scans provided similar high levels of accuracy, with shorter scan times and decreased exposure to ionizing radiation compared to the 1-mm helical scan.[2] Although our data suggest that the helical 1-mm and 3-mm images may have provided better detection sensitivity than did the axial 3-mm scans, especially for FBs smaller than 0.06 mm^3, the small sample size did not provide the necessary statistical power to determine this with certainty.

The smallest IOFB detected in our study was 0.048 mm^3 (Figs 1, 3), 20% smaller than the smallest detectable size reported previously.[1] It is extremely unlikely that particles of this size could be detected reliably by plain films or ultrasound. Although it is improbable that fragments of such low mass could penetrate the eye by themselves, it is possible that FBs of this size could be deposited in the eye by a larger penetrating injury or FB.[2] The accurate detection and localization of such small particles, therefore, remains a clinically relevant issue.

Although FB size seemed to be the predominant factor affecting detection sensitivity, other possible reasons for detection errors were noted. In one instance, the placement of a foreign body in close proximity (1.5 mm) to another in an adjacent sector created the appearance of a single foreign body. In another instance, the position of a foreign body was very close to the medial orbital wall and was partially obscured by the contiguous bone (Fig 4). Although it is possible that appropriate manipulation of the bone–soft tissue rendering would have facilitated detection of these FBs, our study was not designed specifically to address these issues. We only mention them, therefore, as incidental observations and do not use them as a basis of comparison between the scanning protocols.

Localization of FBs as intraocular versus episcleral was quite accurate with each of the scanning methods, a feature that is particularly important when planning possible surgical intervention. Interestingly, most of the errors in localization involved incorrectly localizing IOFBs to the episcleral space, even when particle size was taken into account as a possible confounding factor. The reason for this apparent bias is not clear from the study design or methods and requires additional study for clarification.

In considering the accuracy of localization of the different scanning protocols used in our study, it should be noted that the relatively small size of the FBs may have

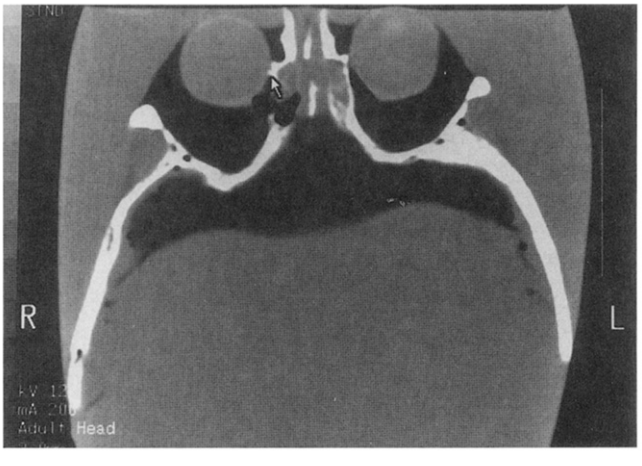

Figure 4. Axial image obtained from a conventional axial scan (3-mm partition, computer reformatted to 1 mm) shows a 0.06-mm^3 extraocular steel foreign body partially obscured by its close proximity to the medial orbital wall bone (arrowhead).

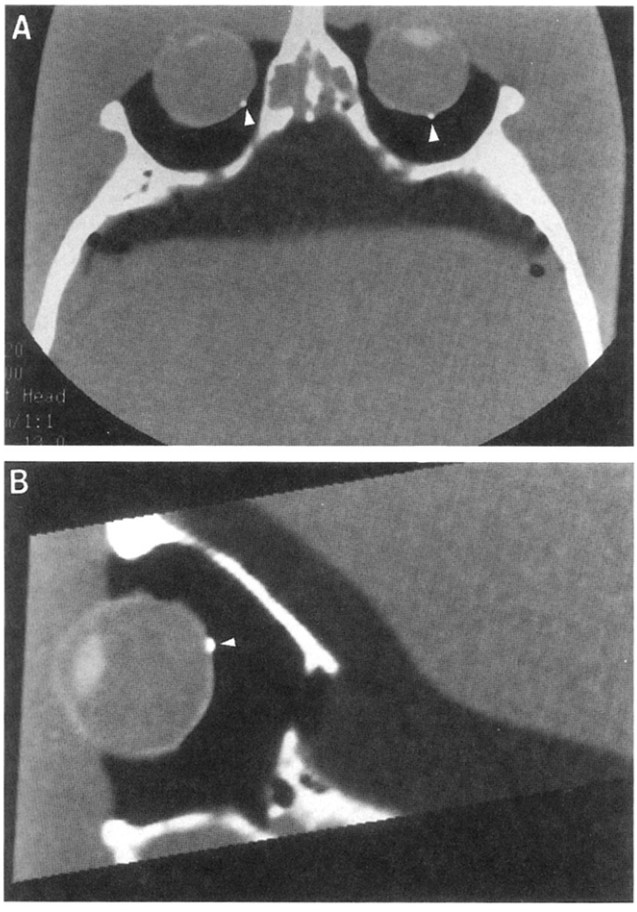

Figure 5. **A**, axial image obtained from helical scan (3-mm partition, 1:1 pitch, computer reformatted to 1 mm) shows foreign bodies in each globe (arrowheads). The size of each foreign body is 0.149 mm^3. **B**, sagittal reconstruction of image data from helical scan in A, shows extraocular location of foreign body adjacent to left globe (arrowhead).

enhanced our ability to localize them, because the metallic *spray* artifact that may occur with larger metallic objects was minimal. This type of artifact, when present, hinders the accurate interpretation of images and may obscure the presence of additional FBs that can be in close proximity.[2] Motion artifact, another potentially significant source of image degradation, also was eliminated in our model system.

Apart from the factors already stated, the actual levels of sensitivity achieved in this study also may be expected to differ from those found in clinical practice because of a number of other potential variables that were not considered in our model. For example, vitreous hemorrhage, bone fragments, and large scleral ruptures conceivably may affect diagnostic accuracy. Similarly, there are numerous soft tissue structures (e.g., blood vessels, lacrimal gland, extraocular muscles) in the orbit that are not represented in our model, which might be expected to influence scan sensitivity and specificity. A potential advantage of helical scanning in this regard is that although both helical and conventional axial scanning techniques yield data that may be computer reformatted at a 3D workstation (Fig 5), only the helical image data can be postprocessed to reduce slice thickness.[9–11] This capability permits a reduction in the volume averaging on the images and might be useful in identifying small FBs. In addition, our model only examined steel FBs. Nonmetallic FBs, which are relatively radiolucent, would not be shown as clearly as the steel fragments used in this study. Finally, because our results are based partly on our use of multiplanar reformatting and postprocessing of image data, they can not be extrapolated directly to a clinical setting in which image analysis typically is confined to the directly acquired images and where direct coronal images also might be obtained.

In summary, our study shows that helical CT scanning, with either 3-mm or 1-mm thick sections and 1:1 pitch, provides a fast, highly sensitive, and specific method of detecting and spatially localizing small steel IOFBs and may be superior to conventional 3-mm axial scanning for this purpose. In addition, the rapid scanning time, seamless data set, and relatively small volume of the eye and orbit make helical CT particularly well suited for evaluation of these structures in the setting of trauma. Although not specifically addressed by our study design, the diagnostic accuracy of the scans appears to be enhanced further by multiplanar reformatting capability and image parameter manipulation.

References

1. Tate E, Cupples H. Detection of orbital foreign bodies with computed tomography: current limits. Am J Neuroradiol 1981;2:363–5.
2. Topilow HW, Ackerman AL, Zimmerman RD. Limitations of computerized tomography in the localization of intraocular foreign bodies. Ophthalmology 1984;91:1086–91.
3. Zinreich SJ, Miller NR, Aguayo JB, et al. Computed tomographic three-dimensional localization and compositional evaluation of intraocular and orbital foreign bodies. Arch Ophthalmol 1986;104:1477–82.
4. Lindhal S. Computed tomography of intraorbital foreign bodies. Acta Radiol 1987;28:235–40.
5. Kelly WM, Paglen PG, Pearson JA, et al. Ferromagnetism of intraocular foreign body causes unilateral blindness after MR study. Am J Neuroradiol 1986;7:243–5.
6. Specht CS, Varga JH, Jalai MM, et al. Orbitocranial wooden foreign body diagnosed by magnetic resonance imaging. Dry wood can be isodense with air and orbital fat by computed tomography. Surv Ophthalmol 1992;36:341–4.
7. Heiken JP, Brink JA, Vannier MW. Spiral (helical) CT. Radiology 1993;189:647–56.
8. O'Brien JM, Char DH, Tucker N, et al. Efficacy of unanesthetized spiral computed tomography scanning in initial evaluation of childhood leukocoria. Ophthalmology 1995;102:1345–50.
9. Napel S. Basic principles of spiral CT. In: Fishman E, Jeffrey R, eds. Spiral CT: Principles, Techniques and Clinical Applications. Chap. 1. New York: Raven Press, 1995.
10. Blumke DA, Fishman EK. Spiral CT of the liver. Am J Radiol 1993;160:787–92.
11. Urban BA, Fishman EK, Kuhlman JE, et al. Spiral CT in the detection of hepatic lesions: the role of 4 mm interscan spacing. Am J Radiol 1993;160:783–5.